

# Coexistence of multi-photon processes and longitudinal couplings in superconducting flux qubits

Yu-xi Liu,<sup>1,2</sup> Cheng-Xi Yang,<sup>3</sup> and Xiang-Bin Wang<sup>3</sup>

<sup>1</sup>*Institute of Microelectronics, Tsinghua University, Beijing 100084, China*

<sup>2</sup>*Tsinghua National Laboratory for Information Science and Technology, Tsinghua University, Beijing 100084, China*

<sup>3</sup>*Department of Physics, Tsinghua University, Beijing 100084, China*

(Dated: November 14, 2019)

In contrast to natural atoms, the potential wells for superconducting flux qubit (SFQ) circuits can be artificially controlled. When the inversion symmetry of the potential energy is broken, it is found that the multi-photon processes can coexist in the multi-level SFQ circuits. Moreover, there are not only transverse but also longitudinal couplings between the external magnetic fields and the SFQs with the broken inversion symmetry. The longitudinal coupling would induce some new phenomena in the SFQs. Here we show that the longitudinal coupling can result in the coexistence of multi-photon processes in the SFQs in analogue to the multi-level SFQ circuits. We also show that the SFQs can become transparent to the transverse coupling fields when the longitudinal coupling fields satisfy the certain conditions. We further show that the quantum Zeno effect can also be induced by the longitudinal coupling in the SFQs. Finally we clarify why the longitudinal coupling can induce coexistence and disappearance of single- and two-photon processes for a driven SFQ, which is coupled to a single-mode quantized field.

PACS numbers: 85.25.Cp, 32.80.Qk, 42.50.Hz.

## I. INTRODUCTION

Superconducting quantum circuits possess discrete energy-levels and behave like natural atoms that the transitions between different energy levels can be induced by the electromagnetic fields. Thus, many experiments realized in natural atoms can also be demonstrated by using the superconducting quantum circuits, e.g., cavity quantum electrodynamics (e.g., in Refs. [1, 2]), dressed states (e.g., in Refs. [3–7]), electromagnetically induced transparency and adiabatic control of quantum states (e.g., in Refs. [8–12]), and cooling for the superconducting qubits (e.g., in Refs. [13–15]), the sideband excitations (e.g., in Refs. [16–18]). In contrast to natural atoms, the potential wells of superconducting flux qubit (SFQ) circuits can be changed by adjusting externally applied magnetic fields, this tunability makes the SFQ circuits have many features which cannot be shown by the nature atoms.

In natural atoms, since the inversion symmetry of the potential energy is given by the nature and cannot be changed artificially. Thus each eigenstate has well-defined parity and the electric-dipole transitions can only link two eigenstates which have different parities. However, the inversion symmetry of the potential energy for the SFQ circuits can be controlled by the external magnetic flux. When the inversion symmetry is adjusted to be broken, there is no well-defined parity for each eigenstate of the multi-level SFQ circuits, and the microwave induced transitions between any two energy levels are possible, thus the multi-photon and single-photon processes can coexist for such multi-level systems. This coexistence of the multi-photon processes can be easily understood by virtue of an example using three-level SFQ circuits. That is, the transition between the ground state and the second excited state can be realized via two different paths: (i) from the ground to the second excited states via a single-photon process; or (ii) from the ground state to the first excited state via a single-photon, and then from the first excited state to the second excited state via another single-photon process [19]. This means that the

single- and two-photon processes can realize the same goal: the transition from the ground to the second excited states, and thus single- and two-photon processes can coexist in such system.

The coexistence [19] of the single- and two-photon processes in the three-level SFQ circuits with the cyclic transition, which is also called as  $\Delta$ -type transition in analogue to the  $\Xi$ -,  $\Lambda$ -, and  $V$ -type transitions in atomic physics or quantum optics [20], has been experimentally demonstrated via a delicate superconducting qubit-resonator circuit [21]. The three-level SFQ circuits with  $\Delta$ -type transitions can be used to generate single photon [22, 23] and cool superconducting qubits [13, 14]. The analysis of the inversion symmetry for the potential energy of the SFQs [19, 24] also shows that one of SFQs cannot be at the optimal point when the frequency matching method is used to control the coupling between two SFQs. Thus an auxiliary circuit or a coupler [16, 25, 26] is necessary to make that both of SFQs can be at their optimal points [16, 24]. Afterwards, several theoretical works [27–30] followed proposals in Refs. [16, 24] and studied how to control two-flux-qubit coupling using an additional nonlinear coupler, which results in experimental studies on the controllable coupling [31] and engineered selection rules for the tunable coupling [32].

Here, we will first explain why the transverse and longitudinal couplings between the microwave fields and the SFQs can coexist, and then mainly focus on some unexplored phenomena resulted from the longitudinal coupling. The transverse coupling between a single-mode microwave field and the SFQ, which can be reduced to the Jaynes-Cummings model in the rotating wave approximation, is well studied in the quantum optics and atomic physics [20]. However, the model with both the transverse and longitudinal couplings is less studied. This is because electric-dipole induced longitudinal coupling does not exist in the natural atoms with well-defined inversion symmetry. But both couplings in the SFQs can coexist when the inversion symmetry of the potential en-

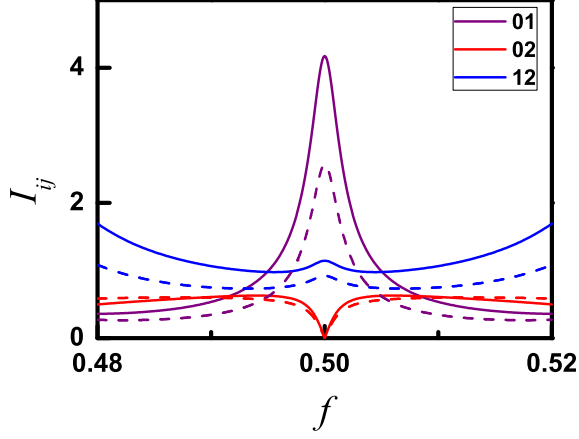


FIG. 1: (Color online) Comparisons of the reduced magnetic flux  $f$ -dependent transition matrix elements  $\langle i|I|j\rangle$  with  $i \neq j$  between the loop current in Eq. (3) with solid curves and that in Refs. [19, 35] with dashed curves for the three lowest energy levels with  $i, j = 0, 1, 2$ . Here, the different transition matrix elements are denoted by different colors as shown in the figure. We take  $\alpha = 0.8$  and  $E_J = 40E_C$  in our numerical simulations.

ergy is broken. Therefore some results, which do not exist in the Jaynes-Cummings model, can be obtained when both couplings coexist. Moreover, we will also study the interaction between the driven SFQs and the low frequency harmonic oscillator [15, 33] when the inversion symmetry of the SFQs is broken.

Our paper is organized as below. In Sec. II, we will briefly review the SFQ circuits. As the complementary and generalization of Ref. [19], we will also clarify some points which were not studied in our earlier literatures. For instance, how to take phase transformations so that the interaction between the SFQ circuits and the external circuit can be described via the product of the loop current of the SFQ circuits and the external magnetic flux, how the multi-photon processes can coexist in  $n$ -level systems when the inversion symmetry is broken. In Sec. III, we will present a Hamiltonian on the transverse and longitudinal couplings between the magnetic fields and the SFQs, and show how the longitudinal coupling can induce the coexistence of multi-photon processes in the SFQs. We will also demonstrate the longitudinal coupling induced dynamical quantum Zeno effect and the transparency of the SFQs to the transverse coupling fields. In Sec. IV, the transverse and longitudinal couplings between the driven SFQ and the low frequency harmonic oscillator (e.g., an LC circuit) is studied. We will explore the nature of the coexistence and disappearance of the single- and two-photon processes in the driven SFQs. Finally, we summary our results in Sec. V.

## II. THEORETICAL MODEL AND COEXISTENCE OF MULTI-PHOTON PROCESSES IN MULTI-LEVEL SFQ CIRCUITS

In this section, we first briefly review the theoretical model on the interaction between the SFQ circuit with three Josephson junctions and the externally applied time-dependent magnetic flux. In the meanwhile, as the complementary and generalization of the results in Ref. [19], we will clarify some points which were not studied in the former literatures (e.g., in Refs. [19, 34]). Then we will summarize the selection rules and discuss the coexistence of multi-photon processes in the multi-level systems.

### A. Hamiltonian and phase transformations

Let us consider a superconducting flux qubit (SFQ) circuit, which is composed of a superconducting loop with three Josephson junctions. As in Ref. [19] and Ref. [34], the two larger junctions are assumed to have equal Josephson energies  $E_{J1} = E_{J2} = E_J$  and capacitances  $C_{J1} = C_{J2} = C_J$ . While for the third junction, the Josephson energy and the capacitance are assumed to be  $E_{J3} = \alpha E_J$  and  $C_{J3} = \alpha C_J$ , with  $\alpha < 1$ . We assume that a static magnetic flux  $\Phi_e$  and a time-dependent magnetic flux  $\Phi(t)$  are applied through the superconducting loop. In this case, the Hamiltonian can be given by

$$H = \frac{P_p^2}{2M_p} + \frac{P_m^2}{2M_m} + U(\varphi_p, \varphi_m) + I\Phi(t). \quad (1)$$

The potential energy  $U(\varphi_p, \varphi_m)$  of the SFQ circuit is defined as

$$U(\varphi_p, \varphi_m) = 2E_J(1 - \cos \varphi_p \cos \varphi_m) + \alpha E_J [1 - \cos(2\pi f + 2\varphi_m)], \quad (2)$$

with the reduced magnetic flux  $f = \Phi_e/\Phi_0$  and the magnetic flux quantum  $\Phi_0$ . The third term  $I\Phi(t)$  in Eq. (1) plays the similar role as the electric-dipole interactions between the nature atoms and the electric fields, and describes the interaction between the SFQ circuit and the time-dependent magnetic flux provided by the external circuit. The parameter  $I$  in Eq. (1) denotes the loop current of the SFQ circuit given by [24]

$$I = \frac{\alpha I_0}{2\alpha + 1} [2 \sin \varphi_p \cos \varphi_m - \sin(2\pi f + 2\varphi_m)], \quad (3)$$

when the time-dependent magnetic flux  $\Phi(t) = 0$ , here  $I_0 = 2\pi E_J/\Phi_0$ . We note that Eq. (3) is different from that in the former literatures (e.g., in Refs. [19, 35]). This difference results from different phase transformations

$$\phi_p = \frac{1}{2}(\phi_1 + \phi_2) + \frac{2\pi\alpha}{(1+2\alpha)} \frac{\Phi(t)}{\Phi_0}, \quad (4)$$

$$\phi_m = \frac{1}{2}(\phi_2 - \phi_1), \quad (5)$$

with the superconducting phase differences  $\phi_1$  and  $\phi_2$  of the two identical Josephson junctions. We also use the phase constraint condition for superconducting phase differences  $\phi_i$  (with  $i = 1, 2, 3$ ) of the three Josephson junctions as

$$-\phi_1 + \phi_2 + \phi_3 + \frac{2\pi\Phi_e}{\Phi_0} + \frac{2\pi\Phi(t)}{\Phi_0} = 0, \quad (6)$$

when Eqs. (2) and (3) are derived.

In the former literatures (e.g., in Refs. [19, 35]), the second term in Eq. (4) for the phase transformations has been neglected, thus  $I$  in Eq. (1) is the supercurrent operator of the third Josephson junction. However, the phase transformations in Eqs. (4) and (5) are more appropriate than that used in former literatures (e.g., in Refs. [19, 35]) when the time-dependent magnetic flux is considered. Because in this transformation, the interaction between the SFQ circuit and the external circuit can be explained by the product of the loop current  $I$  of the SFQ circuit [24] and the external magnetic flux  $\Phi(t)$  provided by the external circuit. This is more reasonable than the product of the supercurrent operator of the third Josephson junction and the external magnetic flux  $\Phi(t)$ .

Physically, the interaction Hamiltonian between the SFQ circuit and the external magnetic flux  $\Phi(t)$  in the former literatures (e.g., in Refs. [19, 35]) is just an approximated result that the displacement currents in the Josephson junctions are simply neglected when the loop current is calculated. Therefore, the loop current is simply taken as one supercurrent of three Josephson junctions. However, here, the interaction Hamiltonian in the fourth term of Eq. (1) is an exact result that the displacement current for each junction is considered when the loop current is calculated.

We should also note that the transformations applied in Eqs. (4) and (5) do not change the basic results on the selection rules and the adiabatic control of the quantum states that were studied in Ref. [19] with neglecting displacement currents. This can be very easily verified by using Eq. (2) and Eq. (3), that is: (i) when  $f = 1/2$  which is called as an optimal point, the potential energy in Eq. (2) is even function of the variables  $\phi_p$  and  $\phi_m$ , the supercurrent in Eq. (3) is the odd function of the variables  $\phi_m$  and  $\phi_p$ , therefore the potential energy and the supercurrent have the well-defined symmetry; (ii) when  $f \neq 1/2$ , the inversion symmetries for both the potential energy and the supercurrent in Eq. (2) and Eq. (3) do not exist. Therefore, when the  $f = 1/2$  or  $f \neq 1/2$ , the conclusions in (a) and (b) are the same as those in Refs. [19, 35]. However due to the different expressions of the loop currents in Eq. (3) and in Refs. [19, 35], the transition matrix elements will be re-normalized. Below we will further clarify this conclusion via the discussions on the selection rules and numerical calculations for the transition matrix elements.

### B. Selection rules and coexistence of multi-photon processes in $n$ -level systems

As necessary supplementary and generalization of the results in Ref. [19] for the microwave induced transitions between two different energy levels, we now rewrite the Hamil-

TABLE I: Comparison between SFQ circuits and natural atoms for dipole moments, parities, symmetry, and selection rules.

Atoms	Dipole moments	Parities	Symmetry	Selection rules
Natural atoms	$\propto e \vec{r}$	Odd	Well-defined	Has
SQC ( $f = 1/2$ )	$\propto -\sin(2\varphi_m) + 2\sin(\varphi_p)\cos(\varphi_m)$	Odd	Well-defined	Has
SQC ( $f \neq 1/2$ )	$\propto -\sin(2\varphi_m + 2\pi f) + 2\sin(\varphi_p)\cos(\varphi_m)$	No parity	Broken	No

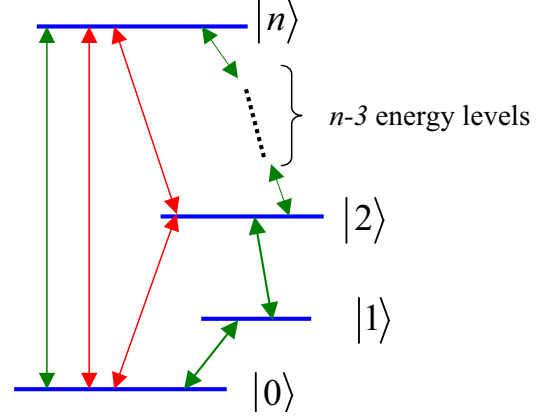


FIG. 2: (Color online) Schematic diagram for the coexistence of different photon transition processes when the inversion symmetry of the potential is broken, i.e.,  $f \neq 1/2$ . In this case, all transitions between any two energy levels are possible, i.e., there is no forbidden transition. For example, the loop formed by three red arrow lines (which link to ground state, the second excited state, and the  $n$ th excited state) denote a coexistence of single- and two-photon processes for the  $n + 1$  level system. Of course, the coexistence of single- and two-photon processes can also be formed by the ground, first excited, and second excited states. However, the loop (formed by the green arrow lines which link the ground, second, third, until  $n$ th excited states) denotes the coexistence of the single- and  $n$ -photon processes for the  $n + 1$  level system. This schematic diagram also shows that many different photon processes can coexist in the SFQ circuit with the broken inversion symmetry.

tonian in Eq. (1) using eigenstates  $\{|i\rangle, i = 0, \dots, n\}$  of the SFQ circuits as the basis

$$H = \sum_i \hbar\omega_{ii}|i\rangle\langle i| + \sum_{i,j=0}^n I_{ij}(f)|j\rangle\langle i|\Phi(t). \quad (7)$$

with “dipole” matrix elements  $I_{ij}(f) = \langle i|I|j\rangle$  and the eigenvalue  $\hbar\omega_{ii}$  of the eigenstate  $|i\rangle$ . Equation (2) clearly shows that the reduced magnetic flux  $f = \Phi_e/\Phi_0$  determines the symmetry of the potential energy of the SFQ circuits.

As discussed above for  $f = 1/2$ , the potential energy in Eq. (2) and the loop current in Eq. (3) have inversion symmetries, and also all eigenstates of the SFQ circuit have well-defined parities. Because the loop current  $I$  in Eq. (3) is an odd function of the variables  $\phi_p$  and  $\phi_m$ , Therefore at the point  $f = 1/2$ , the SFQ circuit has the same selection rules as

the natural atoms, the microwave-induced transition can only link two states which have different parities. However the symmetry is broken when  $f \neq 1/2$ , the selection rules of the SFQ circuits do not exist, the microwave induced transitions between any two energy levels are possible. The comparison of the selection rules between the SFQ circuits and natural atoms is summarized in Table I.

To compare the results on the reduced magnetic flux  $f$ -dependent transition matrix elements using the loop current in Eq. (3) and that in Refs. [19, 35], the transition matrix elements  $\langle i|I|j \rangle$  versus the reduced magnetic flux is plotted in Fig. 1 for the three lowest energy levels with  $i, j = 0, 1, 2$  and  $i \neq j$ . Numerical results in Fig. 1 also clearly show that there are the same transition rules induced by the loop current operator used either in Eq. (3) or in Ref. [19]. However, as shown in Fig. 1, the amplitudes of the transition matrix elements are a little different for two different loop current expressions.

As shown in Table I and Fig. 1, when the inversion symmetry of the potential energy is broken (i.e.,  $f \neq 1/2$ ), all transition matrix elements are not zero, thus the transitions between any two levels are allowed. In this case, the single-photon and  $n$ -photon processes can coexist for a  $(n+1)$ -level SFQ circuit. That is, for a  $n+1$  level system, the transition from the ground state  $|0\rangle$  to the  $n$  excited state  $|n\rangle$  can be realized by either the single-photon process ( $|0\rangle \rightarrow |n\rangle$ ) or the  $n$ -photon processes ( $|0\rangle \rightarrow |1\rangle \rightarrow \dots \rightarrow |n-1\rangle \rightarrow |n\rangle$ ). Similarly, many different photon processes can also coexist in the case with the broken inversion symmetry. The coexistence of single- and  $n$ -photon processes has been schematically shown in Fig. 2. When  $n = 2$ , we have the three-level SFQ circuit as discussed in Ref. [19], then the single- and two-photon can coexist. It should be noted that the transitions between two energy levels should obey the selection rules at the optimal point  $f = 1/2$ . The photon transition processes for the  $(n+1)$ -level SFQ circuit have been schematically shown in Fig. (3) for the case  $f = 1/2$ .

In the above, we mainly complement some analysis on the basic properties of the multi-level SFQ circuits. In view of the big progress for the experimental studies on SFQs [36–39], below we will focus on some unexplored features for the SFQs when the inversion symmetry of the potential energy is broken.

### III. NEW PHENOMENA INDUCED BY LONGITUDINAL COUPLINGS BETWEEN SFQS AND EXTERNAL MAGNETIC FLUXES

#### A. Theoretical model on the couplings between SFQs and time-dependent magnetic fluxes

Let us consider the case of the two energy levels for the SFQs, i.e.,  $n = 1$ , in this case, the Hamiltonian in Eq. (7) is reduced to that of the superconducting flux qubits (SFQs), driven by the time-dependent external magnetic flux. In Fig. 4, the matrix elements of the loop current  $I$  of the SFQs for the two energy levels  $|0\rangle$  and  $|1\rangle$  is plotted versus the re-

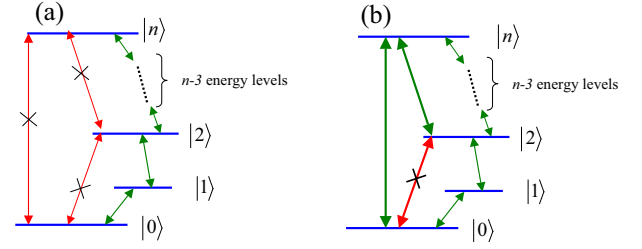


FIG. 3: (Color online) The Schematic diagram for the photon transition processes when the inversion symmetry of the potential energy is well-defined, i.e.,  $f = 1/2$ . For the convenience of the discussions, let us assume that the microwave induced transition between energy levels  $|n\rangle$  and  $|n+1\rangle$  is possible for the  $n+1$  level system. Therefore, it is clear that the transition between the state  $|0\rangle$  and the state  $|2\rangle$  is prohibited. In (a), if the transition between the state  $|2\rangle$  and the state  $|n\rangle$  is prohibited, then the transition between the state  $|n\rangle$  and the state  $|0\rangle$  is also prohibited; In (b), if the transition between the state  $|2\rangle$  and the state  $|n\rangle$  is allowed, then the transition between the state  $|n\rangle$  and the state  $|0\rangle$  is also allowed, however transition between the states  $|0\rangle$  and  $|2\rangle$  is forbidden. In both figures, the sign “x” denotes that the electric-dipole-like microwave induced transition is prohibited. Because the parities for those states are the same.

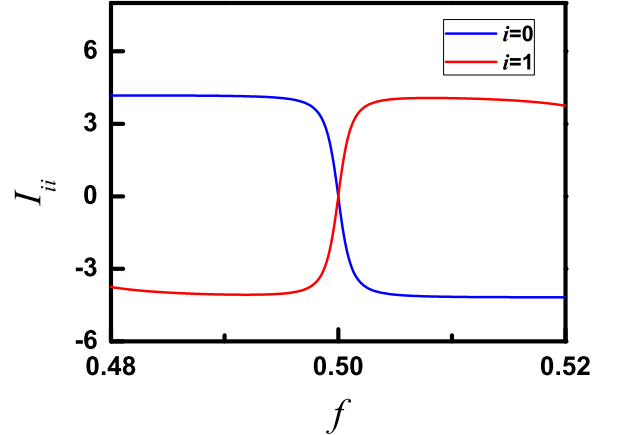


FIG. 4: (Color online) The reduced magnetic flux  $f$ -dependent loop current  $\langle i|I|i \rangle$  for the two lowest eigenstates  $|0\rangle$  and  $|1\rangle$ . Here, we also take the typical numbers  $\alpha = 0.8$  and  $E_J = 40E_c$  in our numerical simulations.

duced magnetic flux  $f$ . Fig. 4 shows a well-known result that the loop current  $I$  in the ground  $|0\rangle$  and the first excited  $|1\rangle$  states are zero at the symmetric point  $f = 1/2$ . However, once the symmetry is broken, the loop current for both states are not zero. Therefore, for a SFQ interacting with the time-dependent magnetic flux, we have the following Hamiltonian

$$H = \sum_{i=0}^1 \hbar \omega_{ii}(f) |i\rangle \langle i| + [I_{01}(f) |0\rangle \langle 1| + I_{10}(f) |1\rangle \langle 0|] \Phi(t) + [I_{00}(f) |0\rangle \langle 0| + I_{11}(f) |1\rangle \langle 1|] \Phi(t). \quad (8)$$

Here, we write  $\omega_{ii}(f)$  and  $I_{ij}(f)$  (with  $i, j = 0, 1$ ) to emphasize the  $f$ -dependent parameters.

Let us now first discuss the interaction between the SFQs and the classical magnetic flux  $\Phi(t)$  using the Hamiltonian in Eq. (8) when  $f = 1/2$ . The above analytical analysis together with Fig. 1 and Fig. 4 show

$$I_{00}(f = 0.5) = I_{11}(f = 0.5) = 0, \quad (9)$$

and

$$I_{10}(f = 0.5) = I_{01}(f = 0.5) \neq 0. \quad (10)$$

Therefore, in Eq. (8), the two coupling terms become into

$$I_{ii}(f = 0.5)|i\rangle\langle i|\Phi(t) = 0, \quad (11)$$

with  $i = 0, 1$ , which means that there is no the longitudinal coupling between the time-dependent magnetic flux and the SFQ at the optimal point. There are only coupling terms  $I_{01}(f = 0.5)(|0\rangle\langle 1| + |1\rangle\langle 0|)\Phi(t)$  in Eq. (8), called as the transverse coupling between the time-dependent magnetic flux and the SFQ. Therefore, under the rotating wave approximation, the Hamiltonian in Eq. (8) at the optimal point can further be reduced to the Jaynes-Cumming model, which has been extensively explored in the quantum optics and the circuit QED system.

When  $f \neq 1/2$ , all elements  $I_{ij}(f)$  with  $i = 0, 1$  are not zero, the interaction Hamiltonian between the time-dependent magnetic flux and the SFQs includes both transverse and longitudinal couplings, which are less studied. This longitudinal coupling can induce some unusual phenomena which will be explored below. For the convenience of the discussions, our studies below just consider the case of the longitudinal and transverse couplings between one driving classical field and the SFQs, however all of discussions in the subsections III B, III C, and III D can be applied to the case with more driving fields.

### B. Longitudinal coupling induced coexistence of multi-photon processes in SFQs

For the convenience of the discussions, using the relations in Eqs. (9) and (10), the Hamiltonian in Eq. (8) can be rewritten as

$$H = \hbar \frac{\omega_q}{2} \sigma_z + \hbar(\lambda_x \sigma_x + \lambda_z \sigma_z) \cos(\omega_0 t), \quad (12)$$

with  $\sigma_z = |1\rangle\langle 1| - |0\rangle\langle 0|$  and  $\sigma_x = |0\rangle\langle 1| + |1\rangle\langle 0|$ . Here, we assume the magnetic flux  $\Phi(t)$  in Eq. (8) to be  $\Phi(t) = \Phi \cos(\omega_0 t)$ , and then  $\lambda_x = \Phi I_{01}$  and  $\lambda_z = \Phi I_{11}$ .

If the SFQ works at the optimal point (i.e.,  $f = 0.5$ ), then  $I_{11}(f = 0.5) = 0$  which implies the longitudinal coupling constant  $\lambda_z = 0$ . In this case, Eq. (12) becomes into a standard Hamiltonian of a driven SFQ, and there is only single-photon resonant transition in the SFQ induced by the external magnetic flux with the condition  $\omega_q = \omega_0$ .

When the reduced magnetic flux deviates from the optimal point, i.e.,  $f \neq 0.5$ , there are both the transverse and longitudinal couplings between the SFQ and the external magnetic

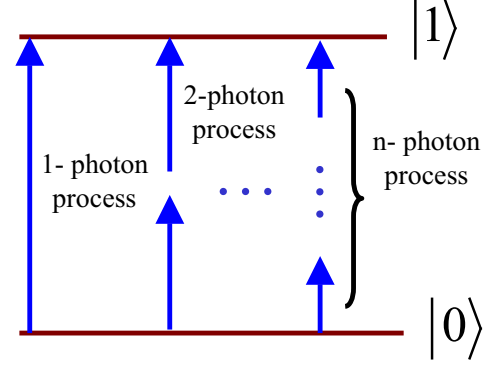


FIG. 5: (Color online) Schematic diagram for the longitudinal coupling induced coexistence of multi-photon processes in the SFQs

flux. In contrast to the case of only the single-photon process for the transverse coupling between the SFQ and the external magnetic flux, the longitudinal coupling can result in the coexistence of the multi-photon processes in the SFQs. To demonstrate this, we now apply a unitary transformation

$$U(t) = \exp \left[ -\frac{i}{2} \left( \omega_0 t + 2 \frac{\lambda_z}{\omega_0} \sin \omega_0 t \right) \sigma_z \right] \quad (13)$$

to Eq. (12), and thus the Hamiltonian in Eq. (12) becomes into

$$H = \hbar \frac{\omega_q - \omega_0}{2} \sigma_z + \hbar \sum_n [\lambda_n e^{-in\omega_0 t} \sigma_+ + \text{h.c.}], \quad (14)$$

under the rotating wave approximation. The effective Rabi frequency in Eq. (14) is given by

$$\lambda_n = \lambda_x J_n \left[ \frac{2\lambda_z}{\omega_0} \right], \quad (15)$$

which depends on both  $\lambda_z$  and  $\omega_0$  with the Bessel functions  $J_n(2\lambda_z/\omega_0)$  of the first kind. When Eq. (14) is derived, we use the relation

$$\exp \left[ i \frac{2\lambda_z}{\omega_0} \sin(\omega_0 t) \right] = \sum_{n=-\infty}^{n=\infty} J_n \left[ \frac{2\lambda_z}{\omega_0} \right] \exp [in\omega_0 t]. \quad (16)$$

We note if the SFQ works at the optimal point, then  $\lambda_z = 0$  and the Bessel functions

$$J_{n \neq 0} \left( \frac{2\lambda_z}{\omega_0} = 0 \right) = 0, \quad (17)$$

$$J_{n=0} \left( \frac{2\lambda_z}{\omega_0} = 0 \right) = 1. \quad (18)$$

In this case, Eq. (14) is reduced to the usual Jaynes-Cumming model for externally driven two-level system, and only describes the single-photon resonant transition with the condition  $\omega_q = \omega_0$ . The single-photon process is characterized by the term for  $n = 0$  in Eq. (14) with the amplitude

$$\lambda_0 = \lambda_x J_0 \left( \frac{2\lambda_z}{\omega_0} = 0 \right) = \lambda_x. \quad (19)$$



This is also a obvious result of Eq. (12) for  $\lambda_z = 0$  and with the rotating wave approximation as described above.

However, for the case  $\lambda_z \neq 0$ , all Bessel functions  $J_n(2\lambda_z/\omega_0)$  and then  $\lambda_n$  are nonzero besides some special ratios of  $2\lambda_z/\omega_0$  which are roots of the Bessel functions. For nonzero  $\lambda_n$ , Eq. (14) shows a obvious resonant condition

$$\omega_q = (n+1)\omega_0. \quad (20)$$

Therefore when the inversion symmetry is broken, the longitudinal coupling can induce the coexistence of the multi-photon processes in the SFQ. The coexistence of the multi-photon processes in the SFQs are schematically shown in Fig. 5.

In summary, the condition for the coexistence of the multi-photon processes in the SFQs is: (a) the SFQs do not work at the optimal point, and thus there is both the longitudinal and transverse couplings between the SFQs and the external magnetic fluxes; (b) the ratios  $2\lambda_z/\omega_0$  are not roots of the function  $J_n(2\lambda_z/\omega_0)$ . The multi-photon processes in the SFQs with the driving fields [40] have been experimentally observed (e.g., in Refs. [41–44]). Thus the above two conditions and our studies here should be necessarily theoretical complementary to these experimental studies (e.g., in Refs. [41–44]).

We also notice that the Hamiltonian used in Eq. (12) is equivalent to one, commonly used in the literatures (e.g., Refs. [41, 42]), described by

$$H' = \varepsilon\sigma_z + \Delta\sigma_x + \lambda\sigma_z \cos(\omega_0 t), \quad (21)$$

in the loop current basis. Because Eq. (21) can be easily transformed to Eq. (12) by using the qubit basis through diagonalizing the first two terms of Eq. (21).

### C. Longitudinal coupling induced transparency of the SFQs to the transverse coupling fields

We now show how the longitudinal coupling field can result in the transparency of the SFQ to the transverse coupling fields. Let us first give the solutions of the Hamiltonian in Eq. (14). We assume that the solutions  $|\Psi\rangle$  of Eq. (14) have the following form

$$|\Psi\rangle = A(t)|0\rangle + B(t)|1\rangle. \quad (22)$$

Because of the expansion with the Bessel functions in the Hamiltonian corresponding to Eq. (14), there are many resonant peaks under the frequency matching condition  $\omega_q = (n+1)\omega_0$ . If we assume that the frequency of the driving field satisfies the condition  $\omega_0 = \omega_q/(n+1)$ , then the time-dependent parameters  $A(t)$  and  $B(t)$  can be given by

$$A(t) = \left\{ A(0) \left[ \cos\left(\frac{\Omega_n t}{2}\right) - i\frac{\Delta_n}{\Omega_n} \sin\left(\frac{\Omega_n t}{2}\right) \right] - iB(0)\frac{2\lambda_n}{\Omega_n} \sin\left(\frac{\Omega_n t}{2}\right) \right\} \exp\left[i\frac{n\omega_0 t}{2}\right] \quad (23)$$

$$B(t) = \left\{ B(0) \left[ \cos\left(\frac{\Omega_n t}{2}\right) + i\frac{\Delta_n}{\Omega_n} \sin\left(\frac{\Omega_n t}{2}\right) \right] - iA(0)\frac{2\lambda_n}{\Omega_n} \sin\left(\frac{\Omega_n t}{2}\right) \right\} \exp\left[-i\frac{n\omega_0 t}{2}\right]. \quad (24)$$

Here,  $A(0)$  and  $B(0)$  are given by the initial conditions of Eq. (22). The Rabi frequency  $\Omega_n$  and the parameter  $\Delta_n$  are given by

$$\Omega_n = \sqrt{\Delta_n^2 + 4|\lambda_n|^2}, \quad (25)$$

$$\Delta_n = \omega_q - (n+1)\omega_0. \quad (26)$$

If the SFQ is initially prepared to the ground state, i.e.,  $A(0) = 1$ , and also the coupling constant  $\lambda_n$  satisfies the condition  $\lambda_n = 0$ , which can be obtained by tuning the ratios  $2\lambda_z/\omega_0$  so that these ratios make  $J_n(2\lambda_z/\omega_0)$  as zero, then from Eqs. (23) and (24), we can obtain  $|B(t)| \equiv 0$  and  $|A(t)| \equiv 1$ . In this case, the SFQ is always in its ground state and the population in the excited state is always zero even that the resonant condition  $\omega_q = (n+1)\omega_0$  is satisfied, this means that the SFQ does not absorb the transverse coupling field and is transparent to the transverse field due to the existence of the longitudinal coupling. However when the longitudinal coupling is the zero, once the resonant condition is satisfied, the transverse field is absorbed by the SFQ.

### D. Longitudinal coupling induced dynamical quantum Zeno effect

We now study another interesting phenomena on how the environmental effect on the flux qubit can be switched off by virtue of the longitudinal coupling field when the inversion symmetry of the SFQ potential energy is broken. The Hamiltonian of the driven SFQ interacting with the environment can be written as

$$H_{\text{en}} = \hbar\frac{\omega_q}{2}\sigma_z + \hbar(\lambda_x\sigma_x + \lambda_z\sigma_z)\cos(\omega_0 t) + \sum_i \hbar\omega_i b_i^\dagger b_i + \hbar \sum_i (g_i\sigma_+ b_i + g_i^*\sigma_- b_i^\dagger), \quad (27)$$

with the definition  $\sigma_x = \sigma_+ + \sigma_-$  for the ladder operators  $\sigma_\pm$ . Here, as in Eq. (12), the longitudinal and transverse couplings between the SFQ and the classical fields are characterized by the parameters  $\lambda_z$  and  $\lambda_x$ . The environment is presented as a set of harmonic oscillators, each with the frequency  $\omega_i$  and the creation operator  $b_i^\dagger$ . The coupling constant between the SFQ and the  $i$ th bosonic mode is denoted by  $g_i$ . If a unitary transformation as in Eq. (13) is applied to the Hamiltonian in Eq. (27), then we have an effective Hamiltonian

$$H_{\text{en}}^{\text{eff}} = \hbar\frac{\omega_q - \omega_0}{2}\sigma_z + \hbar \sum_n [\lambda_n e^{-in\omega_0 t} \sigma_+ + \text{h.c.}] + \sum_i \hbar\omega_i b_i^\dagger b_i + \hbar \sum_n \sum_i (g_i^{(n)} \sigma_+ b + g_i^{(n)*} \sigma_- b^\dagger), \quad (28)$$

with

$$g_i^{(n)} = g_i J_n\left(\frac{2\lambda_z}{\omega_0}\right) \exp[i(n+1)\omega_0 t]. \quad (29)$$

Here,  $J_n(2\lambda_z/\omega_0)$  and  $\lambda_n$  are given in Eq. (15).

It is clear that the SFQ is decoupled from its environment at the zeros of  $J_n(2\lambda_z/\omega_0)$ . Therefore, in contrast to the longitudinal coupling induced transparency, once the SFQ is initially prepared in its excited state, it will not decay to the ground state at these zeros, that is, the dynamical quantum Zeno effect (e.g., in Refs. [45, 46]) occurs. Because at these zeros of the Bessel functions,  $\lambda_n = 0$  and  $g_i^{(n)} = 0$ , thus the interaction between the SFQ and its environment is switched off. If the SFQ is initially prepared in the excited state, i.e.,  $B(0) = 1$ , then  $|B(t)| \equiv 1$  and  $|A(t)| \equiv 0$ . In this case, the SFQ evolves freely and is always in its excited state, which is equivalent to a dynamical quantum Zeno effect [45, 46].

Of course, at these zeros, if the SFQ is initially in a coherent state, then it will also coherently survive with a free evolution, because all the interaction between the SFQs and the external environment has been turned off via the longitudinal coupling.

#### IV. COUPLING BETWEEN A DRIVEN SFQ AND AN LC CIRCUIT WITH LOW FREQUENCY

##### A. Theoretical model

As shown in the red dashed box of Fig. 6, we first consider the interaction between a SFQ and a low frequency LC circuit or a low frequency quantized magnetic field (e.g., Refs. [21, 33]). The Hamiltonian can be given by

$$H_q = \sum_{i=0}^1 \hbar \omega_{ii} |i\rangle \langle i| + \hbar \omega a^\dagger a + M \sqrt{\frac{\hbar \omega}{2L}} \sum_{i,j=0}^1 I_{ij} |j\rangle \langle i| (a + a^\dagger), \quad (30)$$

which can further be written as

$$H_q = \hbar \frac{\omega_q}{2} \sigma_z + \hbar \omega a^\dagger a + (g_1 \sigma_x + g_2 \sigma_z) (a + a^\dagger), \quad (31)$$

with the coefficients

$$g_1 = M \sqrt{\frac{\hbar \omega}{2L}} I_{01}, \quad (32)$$

$$g_2 = M \sqrt{\frac{\hbar \omega}{2L}} I_{11}. \quad (33)$$

Here, we have used the condition  $I_{01} = I_{10}$ . The transverse and longitudinal couplings of the SFQ to the LC circuit are realized via the coupling constants  $g_1$  and  $g_2$ . The analysis of the inversion symmetry of the SFQ potential energy tells us that the longitudinal coupling vanishes (i.e.,  $g_2 = 0$ ) only at the optimal point  $f = 0.5$ , however the transverse coupling is always no zero. Below, we will study the case that both transverse and longitudinal coupling terms are no zero for the reduced magnetic flux  $f \neq 0.5$ .

As in experiments [15, 21] and also theoretical studies in Ref. [33], we now consider that the LC circuit and the SFQ are in the regime of the very large detuning, i.e., the dispersive regime

$$\Delta = \omega_q - \omega \gg |g_1|. \quad (34)$$

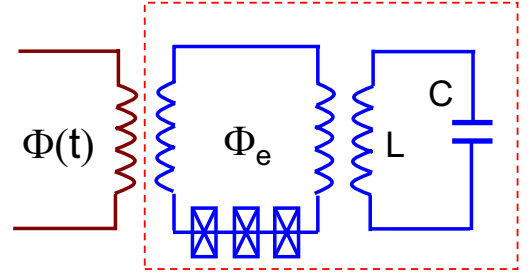


FIG. 6: (Color online) Schematic diagram for the coupling between an LC circuit and the superconducting flux qubit with three Josephson junctions (indicated by the red dashed box), which is driven by the external magnetic flux  $\Phi(t)$  (left part of the figure with the dark red color).

In this condition, for the simplicity of the discussions, we take an approximation

$$\omega_q - \omega \approx \omega_q + \omega, \quad (35)$$

and apply a unitary transformation  $U = \exp(-iS)$  to Eq. (31) with

$$S = \frac{g_1}{\omega_q} (a^\dagger + a) \sigma_y \quad (36)$$

then we have an effective Hamiltonian

$$H_q^{\text{eff}} \approx U^\dagger H_q U = \hbar \frac{\omega_q}{2} \sigma_z + \hbar \omega a^\dagger a + \hbar \sigma_z \left[ g_2 - \frac{g_1^2}{\omega_q} (a^\dagger + a) \right] (a^\dagger + a), \quad (37)$$

which has been obtained in Ref. [33]. Here, we only keep to the first order of  $g_1/\Delta$ . As discussed in Ref. [33], this transform considers that the transverse coupling affects the SFQ via a second-order longitudinal coupling.

##### B. Single- and two-photon coupling between the low frequency oscillator and the driven SFQ

Let us now discuss the coexistence and disappearance of the single and two-photon processes in the driven SFQs when the longitudinal coupling appears. As shown in Fig. 6, we assume that a classical magnetic flux  $\Phi(t)$  with the frequency  $\omega_0$  is applied to the SFQ, which is coupled to an LC circuit. We consider a general case for the reduced magnetic flux  $f \neq 1/2$ , in this case, the classical field has both the transverse and longitudinal couplings to the SFQ via the operators  $\sigma_x$  and  $\sigma_z$ . The total Hamiltonian can be given by

$$H_T = H_q + \hbar(\lambda_x \sigma_x + \lambda_z \sigma_z) \cos(\omega_0 t). \quad (38)$$

As for obtaining Eq. (37), we first apply the unitary transformation  $U = \exp(-iS)$  to Eq. (38), then we obtain an effective Hamiltonian

$$H_T^{\text{eff}} = H_q^{\text{eff}} + \hbar(\lambda_x \sigma_x + \lambda_z \sigma_z) \cos(\omega_0 t). \quad (39)$$

Here, we have neglected the coupling between the LC circuit, the SFQ and the classical magnetic flux by taking a similar approximation as in Ref. [33]. This means  $\omega_q \neq \omega_0 + \omega$ . However, in contrast to the Ref. [33] where only the transverse coupling term is kept, here we keep the both longitudinal and transverse couplings between the classical field and the SFQ. Let us now further apply another unitary transformation

$$U(t) = \exp \left[ \frac{i}{2} \left( \omega_0 t + 2 \frac{\lambda_z}{\omega_0} \sin \omega_0 t \right) \sigma_z \right] \quad (40)$$

to Eq. (39), then we have

$$\begin{aligned} H_T^{\text{eff}} = & \hbar \frac{\omega_q - \omega_0}{2} \sigma_z + \hbar \sigma_z \left[ g_2 + \frac{g_1^2}{\Delta} (a^\dagger + a) \right] (a^\dagger + a) \\ & + \hbar \omega a^\dagger a + \hbar \sum_n [\lambda_n e^{-in\omega_0 t} \sigma_+ + \text{h.c.}] \end{aligned} \quad (41)$$

with the effective Rabi frequency  $\lambda_n = \lambda_x J_n(2\lambda_z/\omega_0)$ . Here, only the term for  $n = 0$  with the amplitude  $\lambda_0 = \lambda_x J_0(2\lambda_z/\omega_0)$  is the time independent.

We assume that the SFQ frequency  $\omega_q$  is near at the frequency  $(n + 1)\omega_0$ , then other fast oscillating terms can be neglected. In the rotating reference frame  $V(t) = \exp(-in\omega_0 \sigma_z t/2)$  and using the dressed SFQ basis, Eq. (41) becomes into

$$H_{T,R}^{\text{eff}} = \hbar \frac{\Omega_R}{2} \sigma_z + \hbar \omega a^\dagger a + \hbar (\beta_1 \sigma_+ a + \beta_2 \sigma_- a^\dagger + \text{h.c.}), \quad (42)$$

with the dressed qubit frequency

$$\Omega_R = \sqrt{[\omega_q - (n + 1)\omega_0]^2 + (2\lambda_n)^2}. \quad (43)$$

Here, the subscript ‘‘R’’ means in the rotating reference frame. We only consider the case that  $\omega = \Omega_R$  or  $2\omega = \Omega_R$ , thus the other fast oscillating terms are neglected. The coupling constants  $\beta_1$  and  $\beta_2$  are

$$\beta_1 = 2 \frac{\lambda_n}{\Omega_R} g_2 \quad (44)$$

$$\beta_2 = 2 \frac{\lambda_n g_1^2}{\Omega_R \Delta} \quad (45)$$

Equation (42) shows that the single-photon process survives when  $\Omega_R = \omega$ , however two-photon process appears when  $\Omega_R = 2\omega$ .

For the single- and two-photon processes in the driven SFQ shown above, we should notice: (i) when the driven SFQ is at the optimal point  $f = 1/2$ , then  $g_2 = 0$  and the Hamiltonian in Eq. (31) is reduced to that of the Jaynes-Cumming model, therefore  $\beta_1 = 0$  in Eq. (42) and only two-photon process exists. However when  $f \neq 1/2$  corresponding to the broken inversion symmetry of the SFQ potential energy, both  $g_1$  and  $g_2$  are not zero, and thus  $\beta_1$  and  $\beta_2$  in Eq. (42) take no zero values, single- and two-photon processes can coexist. (ii) Eq. (42) also shows that both  $\beta_1$  and  $\beta_2$  are proportional to the  $n$ th Bessel functions  $J_n(2\lambda_z/\omega_0)$ . In the case of zeros of the  $n$ th Bessel functions, the transverse coupling via  $\sigma_x$

between the driven SFQ and the LC circuit is switched off, neither single-photon process nor two-photon process can be observed in the driven SFQ. This is an additional condition to obtain the coexistence of the single- and two-photon processes in the driven SFQ [21]. Therefore, the ratio between the longitudinal coupling constant  $\lambda_z$  and the frequency  $\omega_0$  of the driving field determines the coexistence and disappearance of the single- and two-photon processes. (iii) Due to the coexistence of the single- and two-photon processes in the case of the transverse and longitudinal couplings, the preparation and the engineering the quantum states of the harmonic oscillator can be more efficient. (iv) As the closing remark of this section, we also note that the dynamics of the SFQ and the LC oscillator in the dispersive regime beyond the rotating-wave approximation has been studied in Ref. [47]. This method can also be applied to our studies here.

## V. CONCLUSIONS AND DISCUSSIONS

In summary, as the necessary complementary and generalization of our earlier studies [19], we first study physically reasonable phase transformations when the time-dependent microwave is applied, and then study the microwave induced transitions between different energy levels in the multi-level systems formed by the SFQ circuits. We have compared the selection rules between these artificial superconducting ‘‘atoms’’ and the natural atoms. It is found that the selection rules for such multi-level systems are the same as those of the multi-level natural atoms when the reduced bias magnetic flux  $f$ , applied to the superconducting loop of the SFQ circuits, is at the optimal point  $f = 0.5$ . This is because the symmetry of the potential energy is well defined in this case. However, when the reduced bias magnetic flux is not at optimal point, i.e.,  $f \neq 0.5$ , the superconducting ‘‘atoms’’ have no selection rules, in this case, the microwave induced transitions between any two energy levels are possible.

The inversion symmetry of the potential energy for the SFQ circuits is not only important to the multi-level systems, but also important to the two-level systems (qubits). With the broken inversion symmetry, there are both the transverse and longitudinal couplings between the SFQs and the external magnetic fluxes. Comparing with the two-level atoms that only have the transverse coupling, the longitudinal coupling can induce several new results. For example, in the two-level natural atoms, the multiphoton processes cannot coexist due to the well-defined parities of the eigenstates, however, in the SFQs, the longitudinal coupling can induce coexistence of the multiphoton processes. We also demonstrate that the longitudinal coupling can result in: (i) the transparency of the SFQ to the transverse coupling field; (ii) the dynamical quantum Zeno effect.

We further study the coupling between the driven SFQ and the LC circuit with the low frequency. We show that the longitudinal coupling can result in the coexistence of the single- and two-photon processes in contrast to only single-photon process for the case that the longitudinal coupling is zero. We also obtain the conditions that the single- and two-photon



processes can disappear even there is longitudinal coupling. We hope that all of these phenomena can be experimentally demonstrated in the near future by using two-level superconducting quantum circuits.

Finally, we remark: (i) all these results for the SFQs can also be generalized to the superconducting phase [48, 49] and charge [50–53] qubit circuits, because all these qubits have the same Hamiltonians as in Eq. (12) and Eq. (31) when the qubits are not at optimal point. Here, we note that our studies can always be applied the phase qubits which have have no optimal point. (ii) The study on transverse and longitudinal couplings between the superconducting qubit and the LC circuit in the resonant or near-resonant case have been studied, e.g., in Ref. [51], however some new aspects induced by the

longitudinal coupling are still needed to be further explored in the near future.

## VI. ACKNOWLEDGEMENT

Y. X. Liu is supported by the National Natural Science Foundation of China under Nos. 10975080 and 60836001. X. B. Wang is supported by the National Basic Research Program of China grant nos 2007CB907900 and 2007CB807901, NSFC grant number 60725416, and China Hi-Tech program grant no. 2006AA01Z420.

- 
- [1] A. Wallraff, D. I. Schuster, A. Blais, L. Frunzio, R. S. Huang, J. Majer, S. Kumar, S. M. Girvin, and R. J. Schoelkopf, *Nature* **431**, 162 (2004).
  - [2] I. Chiorescu, P. Bertet, K. Semba, Y. Nakamura, C. J. P. M. Harmans, and J. E. Mooij, *Nature* **431**, 159 (2004).
  - [3] Yu-xi Liu, C. P. Sun, and F. Nori, *Phys. Rev.* **74**, 052321 (2006).
  - [4] C. M. Wilson, T. Duty, F. Persson, M. Sandberg, G. Johansson, and P. Delsing, *Phys. Rev. Lett.* **98**, 257003 (2007); C. M. Wilson, G. Johansson, T. Duty, F. Persson, M. Sandberg, and P. Delsing, *Phys. Rev. B* **81**, 024520 (2010).
  - [5] C. Rigetti, A. Blais, and M. Devoret, *Phys. Rev. Lett.* **94**, 240502 (2005).
  - [6] J. M. Fink, R. Bianchetti, M. Baur, M. Goppl, L. Steffen, S. Filipp, P. J. Leek, A. Blais, and A. Wallraff, *Phys. Rev. Lett.* **103**, 083601 (2009).
  - [7] Ya. S. Greenberg, *Phys. Rev. B* **76**, 104520 (2007).
  - [8] K. V. R. M. Murali, Z. Dutton, W. D. Oliver, D. S. Crankshaw, and T. P. Orlando, *Phys. Rev. Lett.* **93**, 087003 (2004); Z. Dutton, K. V. R. M. Murali, W. D. Oliver, and T. P. Orlando, *Phys. Rev. B* **73**, 104516 (2006).
  - [9] M. A. Sillanpää, J. Li, K. Cicak, F. Altomare, J. I. Park, R. W. Simmonds, G. S. Paraoanu, and P. J. Hakonen, *Phys. Rev. Lett.* **103**, 193601 (2009).
  - [10] X. Z. Yuan, H. S. Goan, C. H. Lin, K. D. Zhu, and Y. W. Jiang, *New J. Phys.* **10**, 095016 (2008).
  - [11] H. Ian, Yu-xi Liu, and F. Nori, arXiv:1003.1671.
  - [12] J. Siewert, T. Brandes, and G. Falci, *Phys. Rev. B* **79**, 024504 (2009).
  - [13] J. Q. You, Yu-xi Liu, and F. Nori, *Phys. Rev. Lett.* **100**, 047001 (2008).
  - [14] S. O. Valenzuela, W. D. Oliver, D. M. Berns, K. K. Berggren, L. S. Levitov, and T. P. Orlando, *Science* **314**, 1589 (2006).
  - [15] M. Grajcar, S. H. W. van der Ploeg, A. Izmalkov, E. Il'ichev, H.-G. Meyer, A. Fedorov, A. Shnirman, and G. Schon, *Nature Phys.* **4**, 612 (2008).
  - [16] Yu-xi Liu, L. F. Wei, J. R. Johansson, J. S. Tsai, and F. Nori, *Phys. Rev. B* **76**, 144518 (2007); *cond-mat/0509236*.
  - [17] A. Wallraff, D. I. Schuster, A. Blais, J. M. Gambetta, J. Schreier, L. Frunzio, M. H. Devoret, S. M. Girvin, and R. J. Schoelkopf, *Phys. Rev. Lett.* **99**, 050501 (2007).
  - [18] P. J. Leek, S. Filipp, P. Maurer, M. Baur, R. Bianchetti, J. M. Fink, M. Goppl, L. Steffen, and A. Wallraff, *Phys. Rev. B* **79**, 180511(R) (2009).
  - [19] Yu-xi Liu, J. Q. You, L. F. Wei, C. P. Sun, and F. Nori, *Phys. Rev. Lett.* **95**, 087001 (2005).
  - [20] M. O. Scully and M. S. Zubairy, *Quantum Optics* (Cambridge University Press, Cambridge, England, 1997).
  - [21] F. Deppe, M. Mariani, E. P. Menzel, A. Marx, S. Saito, K. Kakuyanagi, H. Tanaka, T. Meno, K. Semba, and H. Takayanagi, *Nature Phys.* **4**, 686 (2008); T. Niemczyk, F. Deppe, M. Mariani, E. P. Menzel, E. Hoffmann, G. Wild, L. Eggenstein, A. Marx, and R. Gross, *Supercond. Sci. Technol.* **22**, 034009 (2009).
  - [22] J. Q. You, Yu-xi Liu, C. P. Sun, and F. Nori, *Phys. Rev. B* **75**, 104516 (2007).
  - [23] O. Astafiev, K. Inomata, A. O. Niskanen, T. Yamamoto, Yu. A. Pashkin, Y. Nakamura, and J. S. Tsai, *Nature* **449**, 588 (2007).
  - [24] Yu-xi Liu, L. F. Wei, J. S. Tsai, and F. Nori, *Phys. Rev. Lett.* **96**, 067003 (2006).
  - [25] B. L. T. Plourde, J. Zhang, K. B. Whaley, F. K. Wilhelm, T. L. Robertson, T. Hime, S. Linzen, P. A. Reichardt, C.-E. Wu, and J. Clarke, *Phys. Rev. B* **70**, 140501 (2004); B. L. T. Plourde, T. L. Robertson, P. A. Reichardt, T. Hime, S. Linzen, C.-E. Wu, and J. Clarke, *Phys. Rev. B* **72**, 060506(R) (2005).
  - [26] M. Grajcar, A. Izmalkov, S. H. W. van der Ploeg, S. Linzen, E. Il'ichev, Th. Wagner, U. Hubner, H.-G. Meyer, A. M. van den Brink, S. Uchaikin, A. M. Zagorskin, *Phys. Rev. B* **72**, 020503(R) (2005).
  - [27] P. Bertet, C. J. P. M. Harmans, and J. E. Mooij, *Phys. Rev. B* **73**, 064512 (2006).
  - [28] A. O. Niskanen, Y. Nakamura, and J. S. Tsai, *Phys. Rev. B* **73**, 094506 (2006).
  - [29] M. Grajcar, Yu-xi Liu, F. Nori, and A. M. Zagorskin, *Phys. Rev. B* **74**, 172505 (2006).
  - [30] S. Ashhab, A. O. Niskanen, K. Harrabi, Y. Nakamura, T. Picot, P. C. de Groot, C. J. P. M. Harmans, J. E. Mooij, and F. Nori, *Phys. Rev. B* **77**, 014510 (2008).
  - [31] A. O. Niskanen, K. Harrabi, F. Yoshihara, Y. Nakamura, S. Lloyd, and J. S. Tsai, *Science* **316**, 723 (2007).
  - [32] K. Harrabi, F. Yoshihara, A. O. Niskanen, Y. Nakamura, and J. S. Tsai, *Phys. Rev. B* **79**, 020507(R) (2009).
  - [33] J. Hauss, A. Fedorov, C. Hutter, A. Shnirman, and G. Schön, *Phys. Rev. Lett.* **100**, 037003 (2008); J. Hauss, A. Fedorov, S. Andre, V. Brosco, C. Hutter, R. Kothari, S. Yeshwanth, A. Shnirman, and G. Schön, *New J. Phys.* **10**, 095018 (2008).
  - [34] T. P. Orlando, J. E. Mooij, Lin Tian, C. H. van der Wal, L. S. Levitov, S. Lloyd, and J. J. Mazo, *Phys. Rev. B* **60**, 15398 (1999).

- [35] J. Q. You, Y. Nakamura, and F. Nori, Phys. Rev. B **71**, 024532 (2005).
- [36] J. Q. You and F. Nori, Phys. Today **58** (11), 42 (2005).
- [37] R. J. Schoelkopf and S. M. Girvin, Nature **451**, 664 (2008).
- [38] G. Wendin and V. S. Shumeiko, in *Handbook of Theoretical and Computational Nanotechnology*, edited by M. Rieth and W. Schommers (American Scientific, California, 2006), Vol. **3**.
- [39] J. Clarke and F. K. Wilhelm, Nature **453**, 1031 (2008).
- [40] S. Ashhab, J. R. Johansson, A. M. Zagoskin, and F. Nori, Phys. Rev. A **75**, 063414 (2007).
- [41] S. Saito, M. Thorwart, H. Tanaka, M. Ueda, H. Nakano, K. Semba, and H. Takayanagi, Phys. Rev. Lett. **93**, 037001 (2004).
- [42] A. Izmailkov, M. Grajcar, E. Il'ichev, N. Oukhanski, T. Wagner, H.-G. Meyer, W. Krech, M. H. S. Amin, A. Maassen van den Brink, and A. M. Zagoskin, Europhys. Lett. **65**, 844 (2004).
- [43] W. D. Oliver, Y. Yu, J. C. Lee, K. K. Berggren, L. S. Levitov, and T. P. Orlando, Science **310**, 1653 (2005); D. M. Berns, W. D. Oliver, S. O. Valenzuela, A. V. Shytov, K. K. Berggren, L. S. Levitov, and T. P. Orlando, Phys. Rev. Lett. **97**, 150502 (2006).
- [44] X. Wen and Y. Yu, Phys. Rev. B **79**, 094529 (2009).
- [45] A. Peres, Am. J. Phys. **48**, 931 (1980).
- [46] L. Zhou, S. Yang, Yu-xi Liu, C. P. Sun, F. Nori, Phys. Rev. A **80**, 062109 (2009).
- [47] D. Zueco, G. M. Reuther, S. Kohler, and P. Hanggi, Phys. Rev. A **80**, 033846 (2009).
- [48] A. Wallraff, T. Duty, A. Lukashenko, and A. V. Ustinov, Phys. Rev. Lett. **90**, 037003 (2003).
- [49] J. M. Martinis, S. Nam, J. Aumentado, and C. Urbina, Phys. Rev. Lett. **89**, 117901 (2002).
- [50] Y. Nakamura, Yu. A. Pashkin, and J. S. Tsai, Nature **398**, 786 (1999).
- [51] Y. Nakamura, Yu. A. Pashkin, and J. S. Tsai, Phys. Rev. Lett. **87**, 246601 (2001).
- [52] M. Sillanpää, T. Lehtinen, A. Paila, Y. Makhlin, and P. Hakonen, Phys. Rev. Lett. **96**, 187002 (2006).
- [53] A. Aassime, G. Johansson, G. Wendin, R. J. Schoelkopf, and P. Delsing, Phys. Rev. Lett. **86**, 3376 (2001).